Available online at www.sciencedirect.com
ScienceDirect
Journal of Organometallic Chemistry 692 (2007) 3547–3554
Journal of Organometallic Chemistry
www.elsevier.com/locate/jorganchem

Note

Synthesis, structure and cytotoxicity of diorganotin(IV) complexes of 2,6-lutidine-α^2,3-diol (Lu): The crystal structures of Lu and [$SnMe_2(H_2O)$(Lu-2H)]

José S. Casas [a], Alfonso Castiñeiras [a], Félix Condori [a], María D. Couce [b], Umberto Russo [c], Agustín Sánchez [a], José Sordo [a,*], José M[a] Varela [a], Ezequiel M. Vázquez López [b]

[a] Departamento de Química Inorgánica, Facultade de Farmacia, Universidade de Santiago de Compostela, 15782 Santiago de Compostela, Galicia, Spain
[b] Departamento de Química Inorgánica, Facultade de Ciencias, Universidade de Vigo, 36310 Vigo, Galicia, Spain
[c] Dipartimento di Chimica Inorganica, Metallorganica ed Analitica, Università di Padova, Padova, Italy

Received 12 January 2007; received in revised form 20 March 2007; accepted 10 April 2007
Available online 14 April 2007

Abstract

The reaction of dimethyl-, diethyl- and dibutyltin(IV) oxide with 2,6-lutidine-α^2,3-diol (Lu) [2-(hydroxymethyl)-3-hydroxy-6-methylpyridine] in toluene/ethanol has been investigated. The compounds were isolated and characterized by IR, Raman and Mössbauer spectroscopy, EI and FAB mass spectrometry and ^1H and ^{119}Sn NMR spectroscopy. The structures of Lu and [$SnMe_2(H_2O)$(Lu-2H)] were determined by X-ray diffraction. The crystal of [$SnMe_2(H_2O)$(Lu-2H)] contains dimeric [$SnMe_2(H_2O)$(Lu-2H)]$_2$ units, in which the tin atom is coordinated to the O atoms of the two deprotonated hydroxymethyl groups and one deprotonated phenolic hydroxyl group. The distorted octahedral coordination polyhedron of each tin atom is completed by a water molecule and two methyl C atoms. The butyl derivative exhibited significant *in vitro* antitumor activity against the human carcinoma cell lines HeLa-229, A2780 and A2780cis, although minor than that of the pyridoxine derivative prepared previously.

Keywords: Diorganotin(IV) complexes; Lutidine; Pyridoxine; Crystal structure; Antitumor activity

1. Introduction

As part of a broad-ranging project aimed at studying the interaction of diorganotin compounds with vitamins or their derivatives [1], we have previously described the interaction of pyridoxine (PN, vitamin B_6) with the dimethyltin(IV) [2] and diethyltin(IV) [3] cations in the presence of various anions. Furthermore, given the interest in a complete structural characterization of [$SnBu_2$(PN-2H)]$_2$, for which Gielen et al. [4] have demonstrated a significant antitumoral activity against the cellular lines L1210, P815 and P388, and to compare the properties with those of the Me or Et analogues, we reacted the SnR_2O oxides (R = Me, Et, Bu) with pyridoxine [5].

These latter reactions were used to prepare compounds that were structurally characterized and were shown to contain dimeric [SnR_2(PN-2H)]$_2$ units in which bideprotonated pyridoxine (PN-2H) coordinates to tin through the deprotonated phenolic O and the deprotonated O of the C(4)–CH_2OH group, as shown in Scheme 1.

The ligand 2,6-lutidine-α^2,3-diol (Lu) [2-(hydroxymethyl)-3-hydroxy-6-methylpyridine] (Scheme 2) contains, like pyridoxine, adjacent phenolic and hydroxymethyl groups that could lead to a coordination mode similar to that shown by PN-2H, but with the non-coordinated fragment lacking a CH_2–OH group – a situation that would change the biological activity of the complexes. In addition, the hydroxymethyl group is now adjacent to N(1)

* Corresponding author. Tel.: +34 981 528074; fax: +34 981 547102.
E-mail address: qijsordo@usc.es (J. Sordo).

0022-328X/$ - see front matter © 2007 Elsevier B.V. All rights reserved.
doi:10.1016/j.jorganchem.2007.04.004

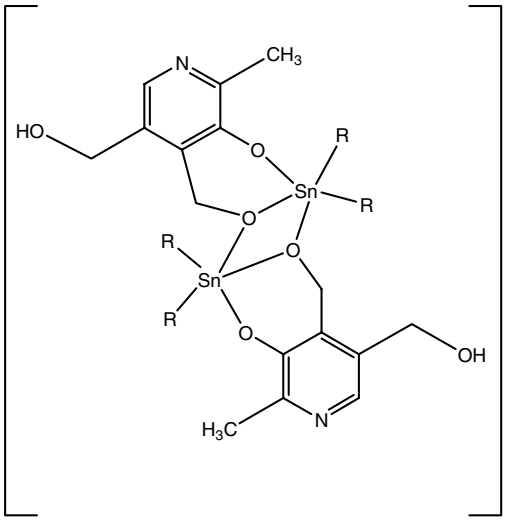

Scheme 1.

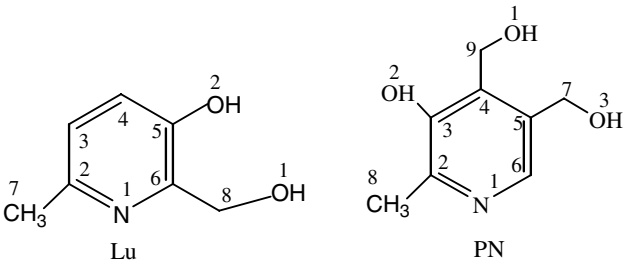

Scheme 2.

and could eventually, once deprotonated, support N-coordination by providing an alternative *N*,*O*-bidentate chelate coordination mode, which would again modify the activity of the compounds.

In order to investigate the coordinative analogies and/or differences between the PN-2H and Lu-2H ligands, and also the different antitumoral activity of the diorganotin(IV) derivatives formed by these two ligands, we reacted 2,6-lutidine-α^2,3-diol (Lu) with diorganotin(IV) oxides (methyl, ethyl and butyl derivatives) using the method previously carried out with PN [5]. The results described here concern the crystal structures of Lu and [$SnMe_2(H_2O)$(Lu-2H)] and a comparative study of the antitumoral activity of [SnR_2(PN-2H)] and [SnR_2(Lu-2H)] (R = Me, Et, Bu) against the cellular lines Hela-229, A2780 and A2780cis.

2. Experimental

2.1. Materials and methods

2,6-Lutidine-α^2,3-diol, dibutyltin oxide (Aldrich) and dimethyltin oxide (Alfa) were used as received. Diethyltin oxide was obtained by treating diethyltin dichloride with sodium hydroxide [6]. Elemental analysis was performed with a Fisons 1108 microanalyser. Melting points were determined with a Büchi apparatus and are uncorrected. Mass spectra were recorded on a Kratos MS50TC spectrometer connected to a DS90 system operating under either EI conditions (direct insertion probe, 70 eV, 250 °C) or in FAB mode (*m*-nitrobenzyl alcohol, Xe, 8 eV; ca. 1.28×10^{-15} J); ions were identified by DS90 software and the intensities of the metallated peaks were calculated using the isotope ^{120}Sn. IR spectra (KBr pellets or Nujol mulls) and Raman spectra (polycrystalline samples) were recorded on a Bruker IFS66V FT-IR spectrophotometer equipped with an FRA-106 Raman accessory and are reported in the synthesis section using the following abbreviations: br = broad, m = medium, s = strong, sh = shoulder, vs = very strong, w = weak. Mössbauer spectra were recorded at 80.0 K in a Harwell cryostat; the $Ca^{119m}SnO_3$ source (15 mCi, NEN) was kept at room temperature and moved with a triangular velocity wave form; suitable computer programs were employed to fit Lorentzian lineshapes to the experimental data. ^{1}H NMR spectra in $CDCl_3$ or MeOD were recorded at room temperature on a Bruker AMX 300 spectrometer operating at 300.14 MHz, using 5 mm o.d. tubes; chemical shifts are reported relative to TMS using the solvent signal (δ ^{1}H = 7.27 or 3.34 ppm) as reference. ^{119}Sn NMR spectra in $CDCl_3$ were recorded at 186.50 MHz on a Bruker AMX 500 spectrometer using 5 mm o.d. tubes and are reported relative to external neat $Sn(CH_3)_4$ (δ^{119}Sn = 0 ppm). Elemental analysis, mass, IR, Raman and NMR spectra and X-ray data were obtained at CACTUS and CACTI, University of Santiago de Compostela (USC) and University of Vigo, respectively.

2.2. Synthesis and characterization of the compounds

2.2.1. Lu

The commercial product was characterized by means of infrared, Raman and ^{1}H NMR spectroscopy. Infrared and Raman (in parentheses), (cm^{-1}): 3097s, br, ν(OH); 1586s (1585 m), 1495s (1495w), ν(ring); 1298s (1291s), ν(C–$O_{phenolic}$); 1012s (1010 m), ν(C–$O_{hydroxymethyl}$). ^{1}H NMR (dmso-d_6, see Scheme 2 for numbering): δ[O(2)H] 9.55s, br(1); δ[C(4)H] 7.05d(1), J = 8.2 Hz; δ[C(3)H] 6.96d(1), J = 8.2 Hz; δ[O(1)H] 4.85s, br(1); δ[C(8)H_2] 4.49s(2); δ[C(7)H_3] 2.34s(3). ^{1}H NMR ($CDCl_3$): δ[C(4)H] 7.06d(1), J = 8.3 Hz; δ[C(3)H] 6.97d(1), δ[C(8)H_2] 4.96s(2); δ[C(7)H_3] 2.45s(3). ^{1}H NMR (MeOD): δ[C(4)H] 7.09d(1), J = 8.3 Hz; δ[C(3)H] 7.01d(1), J = 8.3 Hz; δ[C(8)H_2] 4.70s(2); δ[C(7)H_3] 2.41s(3).

2.2.2. [$SnMe_2$(Lu-2H)] (*1*)

To a solution of Lu (0.50 g, 3.6 mmol) in toluene/absolute ethanol (80:20 v/v, 200 mL) was added solid dimethyltin(IV) oxide (0.60 g, 3.6 mmol). The mixture was heated under reflux for 10 h with water removed by azeotropic distillation using a Dean–Stark apparatus. The solution was concentrated and the resulting oil was treated with petroleum ether. The mixture was stirred for 5 h and the resulting white solid was filtered off and dried in vacuo. Yield 98%. m.p. >250 °C. Anal. Calc. for [$SnMe_2$(Lu-2H)]: C, 37.8; N, 4.9; H, 4.6.

Found: C, 37.1; N, 4.6; H, 5.1%. The main peaks from metallated fragments in the EI spectrum are at *m/e* (ion, intensity): 287 ([$SnMe_2$(Lu-2H)], 100); 257 ([Sn(Lu-2H)], 74.9) and 135 ([SnMe], 64.7). Besides these peaks the EI spectrum shows peaks for the pyridine ring and its fragments, and the FAB spectrum shows peaks for the same metallated species and a signal at 574 ([$SnMe_2$(Lu-2H)]$_2$, 12.2). Infrared and Raman (in parentheses), (cm^{-1}): 1564s, (1589m), 1459vs, (1452w), ν(ring); 1297vs, br(1297m), ν(C–$O_{phenolic}$); 1083vs, ν(C–$O_{hydroxymethyl}$); 563m, (560m), ν_{asym}(Sn–C); 532m, br, (515vs), ν_{sym}(Sn–C). Mössbauer: IS 1.35, QS 3.29, Γ 1.05 mm s^{-1}, $A_{2/1}$ 1.04. ^{1}H NMR ($CDCl_3$): δ[C(4)H; C(3)H] 6.95s, br(2); δ[C(8)H_2] 4.88s(2); δ[C(7)H_3] 2.41s(3); δ[CH_3-Sn] 0.76s(6). ^{1}H NMR (MeOD): δ[C(4)H, C(3)H] 7.05s(2); δ[C(8)H_2] (not observed, included in the water solvent signal); δ[C(7)H_3] 2.41s(3); δ[CH_3-Sn] 0.68s(6), $^2J(^1H–^{119}Sn) = 81.7$ Hz. ^{119}Sn ($CDCl_3$): δ −245.5, −289.0. Crystallization from methanol afforded crystals that were shown by X-ray diffraction to be [$SnMe_2$(H_2O)(Lu-2H)]-(**1** · H_2O).

2.2.3. [$SnEt_2$(Lu-2H)] (**2**)

To a solution of Lu (0.50 g, 3.6 mmol) in toluene/absolute ethanol (80:20 v/v, 200 mL) was added solid diethyltin(IV) oxide (0.69 g, 3.6 mmol). The mixture was heated under reflux for 10 h with water removed by azeotropic distillation using a Dean–Stark apparatus. The solution was concentrated and the resulting oil was treated with petroleum ether. The mixture was stirred for 5 h and the resulting white solid was filtered off and dried in vacuo. Yield 95%. m.p. 220 °C. Anal. Calc. for [$SnEt_2$(Lu-2H)]: C, 42.1; N, 4.5; H, 5.5. Found: C, 41.8; N, 4.3; H, 5.5.%. The main peaks from metallated fragments in the EI spectrum are at *m/e* (ion, intensity): 315 ([$SnEt_2$(Lu-2H)], 68.3); 286 ([SnEt(Lu-2H)], 12.7); 256 ([Sn(Lu-3H)], 100); 178 ([$SnEt_2$], 25.4); 149 ([SnEt], 36.7) and 120 ([Sn], 30.3). Besides these peaks the EI spectrum shows peaks for the pyridine ring and its fragments, and the FAB spectrum shows peaks for the same metallated species and a signal at 630 ([$SnEt_2$(Lu-2H)]$_2$, 7.5). Infrared and Raman (in parentheses), (cm^{-1}): 1564vs, (1589 m), 1459vs, (1456 m), ν(ring); 1298vs, (1298 m), ν(C–$O_{phenolic}$); 1084vs, ν(C–$O_{hydroxymethyl}$); 530vs, (528w), ν_{asym}(Sn–C); 485w, (493vs), ν_{sym}(Sn–C). Mössbauer: IS 1.31, QS 2.85, Γ 1.01 mm s^{-1}, $A_{2/1}$ 0.96. ^{1}H NMR ($CDCl_3$): δ[C(4)H] 6.99d(1); $J = 8.2$ Hz; δ[C(3)H] 6.93d(1); $J = 8.3$ Hz; δ[C(8)H_2] 4.91s(2); $^3J(^1H–^{119}Sn) = 36.4$ Hz; δ[C(7)H_3] 2.40s(3); δ[CH(α)–Sn] 1.48m(4); δ[CH(β)–Sn] 1.29t(6) $^3J(^1H–^{119}Sn) = 123.6$ Hz; ^{1}H NMR (MeOD): δ[C(4)H, C(3)H] 7.05s, br(2); δ[C(8)H_2] (not observed, included in the water solvent signal); [C(7)H_3] 2.39s, br(3); δ[CH(α)-Sn] 1.47s, br(4); [CH(β)–Sn] 1.27t(6). ^{119}Sn ($CDCl_3$): δ −236.8, −270.5.

2.2.4. [$SnBu_2$(Lu-2H)] (**3**)

To a solution of Lu (0.50 g, 3.6 mmol) in toluene/absolute ethanol (80:20 v/v, 200 mL) was added solid dibutyltin(IV) oxide (0.89 g, 3.6 mmol). The mixture was heated under reflux for 10 h with water removed by azeotropic distillation using a Dean–Stark apparatus. The solution was concentrated and the resulting oil was treated with petroleum ether. The mixture was stirred for 5 h and the resulting white solid was filtered off and dried in vacuo. Yield 98%. m.p. 210 °C. Anal. Calc. for [$SnBu_2$(Lu-2H)]: C, 48.6; N, 3.8; H, 6.8. Found: C, 48.6; N, 3.8; H, 7.7%. The main peaks from metallated fragments in the EI spectrum are at *m/e* (ion, intensity): 742 ([$SnBu_2$(Lu-2H)]$_2$, 9.7); 371 ([$SnBu_2$(Lu-2H)], 100); 256 ([Sn(Lu-3H)], 93.1); 177 ([SnBu], 9.3) and 120 ([Sn], 16.9). Besides these peaks the EI spectrum shows peaks for the pyridine ring and its fragments, and the FAB spectrum shows peaks for the same metallated peaks. Infrared and Raman (in parentheses), (cm^{-1}). 1565s, (1590s), 1461vs, ν(ring); 1302vs, (1305 m), ν(C–$O_{phenolic}$); 1086vs, ν(C–$O_{hydroxymethyl}$). Mössbauer: IS 1.31, QS 2.43, Γ 0.89 mm s^{-1}, $A_{2/1}$ 1.04. ^{1}H NMR ($CDCl_3$): δ[C(4)H] 6.97d(1); $J = 8.2$ Hz; δ[C(3)H] 6.93d (1); $J = 8.3$ Hz; δ[C(8)H_2] 4.88s(2); $^3J(^1H–^{119}Sn) = 36.8$ Hz; δ[C(7)H_3] 2.39s(3); δ[CH(α)–Sn] 1.48t(4); δ[CH(β)–Sn] 1.64 m(4); δ[CH(γ)–Sn] 1.36 m(4); δ[CH(δ)–Sn] 0.87t(6); ^{1}H NMR (MeOD): δ[C(4)H, C(3)H]] 7.05s(2); δ[C(8)H_2] 4.85s(2); $^3J(^1H–^{119}Sn) = 36.7$ Hz; [C(7)H_3] 2.38s(3); δ[CH(α)–Sn] 1.51 m(4); δ[CH(β)–Sn] 1.62 m(4); δ[CH(γ)-Sn] 1.35 m(4); δ[CH(δ)-Sn] 0.86t(6). ^{119}Sn ($CDCl_3$): δ −271.3, −331.9.

2.3. Crystal structure determination

2.3.1. X-ray data collection and reduction

Crystals were mounted on glass fibres for data collection on a Bruker CCD Smart automatic diffractometer. Data were collected at 293 K using Mo Kα radiation (λ = 0.71073 Å) and the ω scan technique, and were corrected for Lorentz and polarization effects [7]. MultiScan (SADABS) [8a] or psi scan [8b] semi-empirical absorption corrections were also made.

2.3.2. Structure solution and refinement

The structure was solved by direct methods [9] and subsequent Fourier maps, and refined on F^2 by a full-matrix least-squares procedure using anisotropic displacement parameters [10]. All hydrogen atoms were located from difference Fourier maps and refined as riders [10]. Atomic scattering factors were taken from International Tables for X-ray Crystallography [11]. Molecular graphics were generated with PLATON 99 [12] and PLATON 98 [13]. The crystal data, experimental details and refinement results are summarized in Table 1.

2.4. In vitro antitumor activity

2.4.1. Cell lines and growth conditions

The antitumor tests were performed in HeLa cell cultures from human cervix carcinoma cells (HeLa-229, kindly provided by Dra. Guadalupe Mengod, CSIC-IDIB-

Table 1
Crystal data collection and structure refinement parameters

	Lu	$[SnMe_2(H_2O)$-(Lu-2H)]
Empirical formula	$C_7H_9NO_2$	$C_{18}H_{30}N_2O_6Sn_2$
Formula weight	139.15	607.82
Wavelength (Å)	0.71073	0.71073
Crystal system	Monoclinic	Triclinic
Space group	$P2_1/n$ (no. 14)	$P\bar{1}$ (no. 2)
Unit cell dimensions		
a (Å)	8.0624(13)	8.6328(11)
b (Å)	7.4367(11)	8.901(2)
c (Å)	12.0221(19)	9.4499(17)
α (°)		66.449(16)
β (°)	102.515(3)	81.945(12)
γ (°)		61.540(11)
V, Å^3	703.69(19)	584.1(2)
Z	4	1
D_c (Mg cm^{-3})	1.313	1.728
$F(000)$	296	300
μ (mm^{-1})	0.097	2.171
Crystal size (mm)	$0.29 \times 0.26 \times 0.20$	$0.36 \times 0.20 \times 0.10$
θ Range for data collection (°)	2.79–28.01	2.36–27.97
θ Range (25 reflections) (°)	$28.01 < \theta < 96.2$	$27.97 < \theta < 100.0$
Index ranges	$-7 \leqslant h \leqslant 10$, $-9 \leqslant k \leqslant 7$, $-15 \leqslant l \leqslant 15$	$-0 \leqslant h \leqslant 11$, $-10 \leqslant k \leqslant 11$, $-12 \leqslant l \leqslant 12$
Reflections collected	4151	3004
Unique reflections [R_{int}]	1642 [0.0408]	2818 [0.0166]
Absorption correction	Empirical	Psin-scan
Minimum and maximum transmission	1.000000, 0.502871	0.979, 0.796
Data, restrainst, parameters	1642, 0, 99	2818, 0, 154
Goodness-of-fit on F^2	0.923	1.057
Final R indices [$I > 2\sigma(I)$]	$R_1 = 0.0482$, $wR_2 = 0.1133$	$R_1 = 0.0250$, $wR_2 = 0.0621$
R indices (all data)	$R_1 = 0.0907$, $wR_2 = 0.1276$	$R_1 = 0.0399$, $wR_2 = 0.0659$
Largest difference peak, hole (e Å^{-3})	0.153, −0.183	0.499, −0.816

APS, Barcelona, Spain) and A2780 and A2780cis (from human ovary carcinoma cell lines). The cells were cultured at 37 °C in DMEM (Dulbecco's Modified Eagle's Medium, Sigma-RBI, Spain) supplemented with 10% foetal calf serum (FCS) (Sigma-RBI, Spain) (HeLa-229) and RPMI 1640 supplemented with 10% foetal bovine serum (FBS), and 2 mM L-glutamine (Sigma-RBI, Spain) (A2780, A2780cis) in a humidified atmosphere containing 5% CO_2. The cells were harvested using trypsin-EDTA (Sigma-RBI, Spain).

2.4.2. In vitro chemosensitivity assay

The cells were seeded into 96-well plates (Beckton–Dickinson, Spain) in a volume of 100 μL at a level of 4000 cells/well. After attachment to the culture surface, the cells were incubated for 4–6 h (HeLa-229 cell line) or 24 h (A2780 and A2780cis cell lines). The lutidine and pyridoxine ligands and their tin complexes were dissolved in a maximum of 1% ethanol per well and were added to the cells at concentrations between 0 and 10 μM. After the appropriate incubation time the cells were fixed by adding 10 μL of 11% glutaraldehyde per well for 15 min. The fixative was removed and wells were washed four times with distilled water. Cell biomass was determined by a crystal violet staining technique [14].

The inhibitory potency and the compound concentration able to inhibit cell growth by 50% with respect to the control (IC_{50}) were then determined from semilogarithmic dose–response plots using GraphPad Prism 2.01 software (GraphPad Software Inc.).

For comparison purposes, the cytotoxicity of cisplatin was evaluated under the same experimental conditions. All compounds were tested in two independent studies with quadruplicate points. The *in vitro* studies were performed at the Screening Unit of the Institute for Industrial Pharmacy of the USC.

3. Results and discussion

3.1. Synthesis

The complexes $[SnR_2(Lu\text{-}2H)]$ were synthesized by reacting the appropriate oxide SnR_2O (R = Me, Et and Bu) with 2,6-lutidine-α^2,3-diol in a 1:1 molar ratio, as described in Section 2. The mass spectra (EI mode) showed the molecular ions for all compounds and the FAB spectra showed the signal for the dimers (also present in the EI spectrum for the butyl derivative) along with those for the organotin fragments.

Crystals suitable for X-ray diffraction were obtained by recrystallization of Lu and **1** from methanol; complex **1** acquires H_2O in this process to give $[SnMe_2(H_2O)(Lu\text{-}2H)]$ (**1** · H_2O).

3.2. Solid state structures

3.2.1. Lu

The structure of the compound is shown in Fig. 1 along with the numbering scheme used. Selected bond lengths and angles are listed in Table 2.

As observed in pyridoxine [15], the lutidine ligand exists in the non-zwitterionic form; This fact is supported by the angle C(2)–N(1)–C(6) (120.13(13)°), which confirms the presence of the non-protonated pyridine ring. The N(1)–C(6) ring is planar (r.m.s. = 0.0028) and the O(2), C(7) and C(8) atoms are 0.011(3), 0.035(3) and 0.018(3) Å away from this plane.

The molecular packing in the crystal structure is dominated by hydrogen bonds that involve the N atom, the C(5)–O(2)–H and the C(6)–CH_2–O(1)H. As shown in Fig. 2, the N(1) atom and the O(1)–H hydroxyl group on C(8) are bonded, leading to association of the molecules to form centrosymmetric dimers [O(1)–H(1)···N(1)$^{\#1}$: 0.90(2), 1.83(2); 2.732(1)] Å 173(2)°: symmetry operation: $^{\#1}$: $-x, -y+1, -z$]. The other hydrogen bond includes the C(5)–O(2)–H phenolic group as the hydrogen bond donor and the hydroxyl O(1) atom as the acceptor

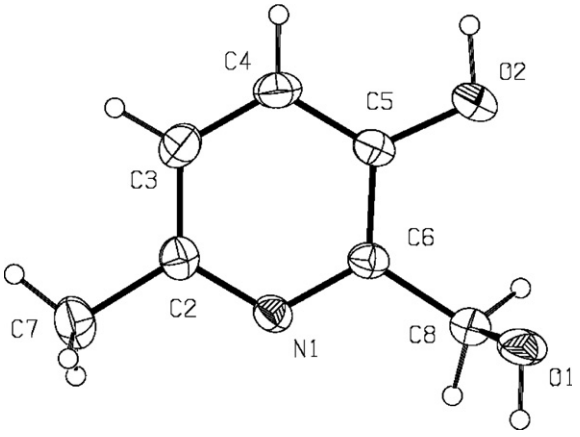

Fig. 1. The molecular structure of Lu, showing the numbering scheme.

Table 2
Bond lengths (Å) and angles (°) in Lu, with e.s.d.'s in parentheses

Bond	
N(1)–C(2)	1.338(2)
N(1)–C(6)	1.3411(19)
C(2)–C(3)	1.385(2)
C(2)–C(7)	1.502(2)
C(3)–C(4)	1.373(3)
C(4)–C(5)	1.382(3)
C(5)–O(2)	1.355(2)
C(5)–C(6)	1.389(2)
C(6)–C(8)	1.497(2)
C(8)–O(1)	1.421(2)
Angle	
C(2)–N(1)–C(6)	120.13(13)
N(1)–C(2)–C(3)	120.59(16)
N(1)–C(2)–C(7)	117.55(15)
C(3)–C(2)–C(7)	121.84(16)
C(4)–C(3)–C(2)	119.99(17)
C(3)–C(4)–C(5)	119.20(16)
O(2)–C(5)–C(4)	124.46(15)
O(2)–C(5)–C(6)	116.99(16)
C(4)–C(5)–C(6)	118.55(16)
N(1)–C(6)–C(5)	121.53(16)
N(1)–C(6)–C(8)	117.79(14)
C(5)–C(6)–C(8)	120.67(15)
O(1)–C(8)–C(6)	111.81(15)

[O(2)–H(2)···O(1) $^{\#2}$: 0.95(3), 1.72(3); 2.639(1)] Å 163(2)°: symmetry operations: $^{\#2}$ $-x-1/2,\ y-1/2,\ -z+1/2$] and leads to these dimers being arranged in sheets along the crystal.

3.2.2. $[SnMe_2(H_2O)(Lu\text{-}2H)]$ ($\mathbf{1}\cdot H_2O$)

The structure consists of dimeric $[SnMe_2(H_2O)(Lu\text{-}2H)]_2$ units in which the bideprotonated 2,6-lutidine-α^2, 3-diol ligand is bound to the metal through its adjacent phenolic and CH_2OH groups, both of which are deprotonated. The structure of the dimeric unit is shown in Fig. 3 along with the numbering scheme used. Selected bond lengths and angles are listed in Table 3. This type of coordination gives rise to the formation of a flat Sn_2O_2 ring as the central element of the structure. In the

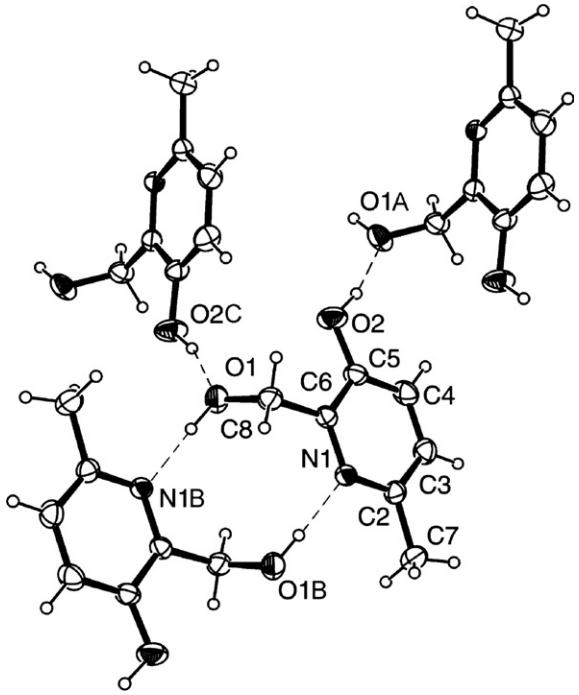

Fig. 2. Packing arrangement in crystalline Lu, showing the hydrogen bonds.

ring, each tin atom is bound to two carbon atoms of the methyl groups, to the O(2) phenolic atom, to the O(1) and O(1)$^{\#1}$ atoms of the hydroxymethyl groups and to an O(3) atom of a water molecule. The resulting tin coordination geometry can be described as distorted octahedral. The principal distortion is due to the Sn_2O_2 ring imposing O–Sn–O angles that are appreciably less than 90°, as is the case for O(1)–Sn(1)–O(1)$^{\#1}$, which has a value of 70.16 (9)°. This Sn_2O_2 central ring is planar (r.m.s.: 0.0032) and the distances and angles in it are close to those found in Sn_2O_2 rings in which hydroxyl O atoms bridge between two $SnMe_2^{2+}$ units [16,17]. The Sn_2O_2 plane makes a dihedral angle of 36.4(1)° with the plane of the N(1)–C(6) ring.

This structure resembles those of $[SnMe_2(H_2O)(PN\text{-}H)]\cdot Cl\cdot H_2O$ and $[SnMe_2(H_2O)(PN\text{-}2H)]\cdot 0.5H_2O$ [2] in which each tin atom has an SnC_2O_4 kernel that adopts a similar distorted octahedral geometry. An inverse relationship was observed with regard to the Sn–O (water) distance (2.963(5), 2.490(2) and 2.466(3) Å, respectively, for the PN-2H, Lu-2H and PN-H derivatives) and the C–Sn–C angle (142.2(2)°, 151.86(17)° and 159.9(1)° for the same compounds) and the present structure corresponds to the intermediate position. Though not so closely related, comparison can also be made with $[SnMe_2(HTDP)(H_2O)]\cdot Cl\cdot H_2O$ (HTDP = thiamine diphosphate) [18] and with $[Sn(n\text{-}Bu)_2(OH)(CF_3SO_3)(H_2O)]_2$ [19]. In the former, the lengths of the Sn–O bonds [2.062(3)–2.586(4) Å, the longest being $Sn–O_{water}$] are similar to those found in $\mathbf{1}\cdot H_2O$ [2.086(2)–2.490(2) Å], but in the latter the range is 2.085(3)–2.622(2) Å, with an $Sn–O_{water}$ distance well inside this range [2.409(3) Å], and in $[Sn(n\text{-}Bu)_2(OH)(CF_3SO_3)$-

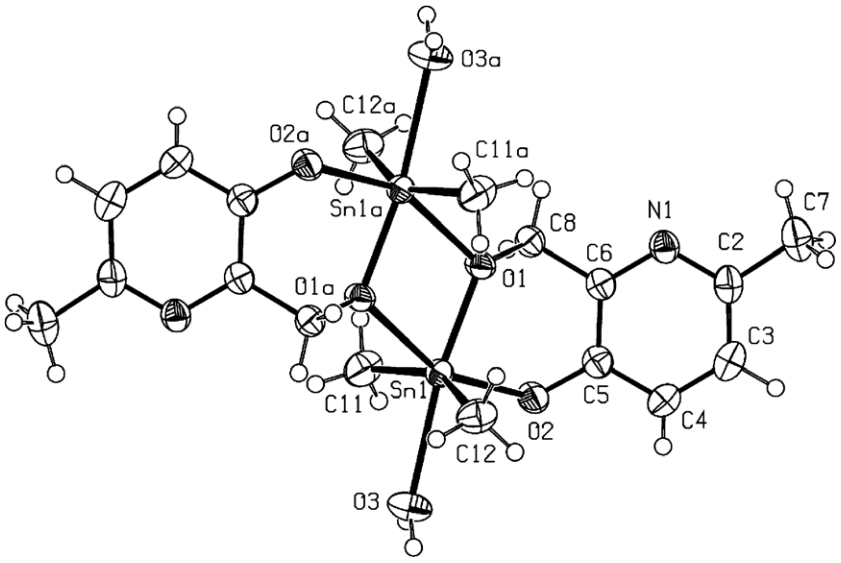

Fig. 3. The molecular structure of $[SnMe_2(H_2O)(Lu\text{-}2H)]$ ($\mathbf{1} \cdot H_2O$), showing the numbering scheme.

Table 3
Bond lengths (Å) and angles (°) in $[SnMe_2(H_2O)(Lu\text{-}2H)]$, with e.s.d.'s in parentheses[a]

(a) Tin environment			
Sn(1)–O(1)	2.086(2)	Sn(1)–C(11)	2.095(3)
Sn(1)–O(2)	2.109(2)	Sn(1)–O(1)#1	2.301(2)
Sn(1)–C(12)	2.110(3)	Sn(1)–O(3)	2.490(2)
O(1)–Sn(1)–O(2)	85.18(8)	O(2)–Sn(1)–C(12)	98.95(13)
O(1)–Sn(1)–C(12)	102.68(12)	C(11)–Sn(1)–C(12)	151.86(17)
O(1)–Sn(1)–C(11)	101.73(13)	C(11)–Sn(1)–O(2)	96.84(13)
O(1)–Sn(1)–O(1)#1	70.16(9)	C(11)–Sn(1)–O(1)#1	86.55(12)
O(2)–Sn(1)–O(1)#1	155.25(8)	C(12)–Sn(1)–O(1)#1	88.73(12)
O(1)–Sn(1)–O(3)	168.76(9)	C(11)–Sn(1)–O(3)	77.64(13)
O(2)–Sn(1)–O(3)	83.77(9)	C(12)–Sn(1)–O(3)	81.09(12)
O(1)#1–Sn(1)–O(3)	120.78(9)	C(8)–O(1)–Sn(1)	119.96(18)
C(8)–O(1)–Sn(1)#1	125.18(18)	Sn(1)–O(1)–Sn(1)#1	109.84(9)
C(5)–O(2)–Sn(1)	121.79(18)	Sn(1)–O(3)–H(3A)	115(3)
(b) 2,6-Lutidine-α,3-diol			
C(8)–O(1)	1.423(4)	C(2)–C(7)	1.506(5)
C(5)–O(2)	1.349(4)	C(3)–C(4)	1.391(5)
N(1)–C(6)	1.343(4)	C(4)–C(5)	1.389(5)
N(1)–C(2)	1.343(4)	C(5)–C(6)	1.399(4)
C(2)–C(3)	1.383(5)	C(6)–C(8)	1.499(4)
C(6)–N(1)–C(2)	119.3(3)	O(2)–C(5)–C(6)	121.3(3)
N(1)–C(2)–C(3)	121.0(3)	C(4)–C(5)–C(6)	117.6(3)
N(1)–C(2)–C(7)	116.6(3)	N(1)–C(6)–C(5)	122.8(3)
C(3)–C(2)–C(7)	122.4(3)	N(1)–C(6)–C(8)	118.4(3)
C(2)–C(3)–C(4)	120.1(3)	C(5)–C(6)–C(8)	118.8(3)
C(5)–C(4)–C(3)	119.1(3)	O(1)–C(8)–C(6)	111.0(2)
O(2)–C(5)–C(4)	121.1(3)		

[a] Symmetry operations: #1 $-x$, $-y$, $-z$.

$(H_2O)]_2$ co-crystallized with $[Sn(n\text{-}Bu)_2(OH)(CF_3SO_3)]_2$ [20] the difference is even greater [range 2.064(4)–2.863(3) Å, $Sn–O_{water} = 2.364(5)$ Å].

Comparison of the geometric parameters of the Lu-2H fragment in the complex with those of free Lu shows that the deprotonation of the phenolic hydroxyl group and the O(2) coordination do not significantly change the C(5)–O(2) bond distance [1.355(2) vs. 1.349(4) Å] and only slightly affect the O(2)–C(5)–C(4) and O(2)–C(5)–C(6) angles [124.46(15) and 116.99(16)° in Lu; 121.1(3) and 121.3(3) in $\mathbf{1} \cdot H_2O$]. Furthermore, the C(8)–O(1) bond distance does not change significantly [1.421(2) vs. 1.423(4)] and neither does the O(1)–C(8)–C(6) bond angle [111.81 (15) vs. 111.0(2)°]. The ring parameters also remain essentially unchanged.

3.3. Spectroscopic studies

The main IR and Raman bands of 2,6-lutidine-α^2,3-diol (Lu) were assigned on the basis of our previous work on pyridoxine [2,3,5]. The spectra of the complexes show that the ν(OH) band present in the spectrum of the ligand disappears as a result of the deprotonation and coordination and the ν(C–O) band of the hydroxymethyl group is shifted to higher wavenumbers. All of the spectra show a strong IR band, medium in Raman, attributed [21] to the ν(C–O) of the coordinated deprotonated phenolic group. As shown in the Experimental part, the positions of the Lu-2H bands in the spectra of the three complexes are similar, suggesting a similar coordinative behaviour for this ligand in all cases. For **1** and **2** both the ν_{as}(Sn–C) and ν_{sym}(Sn–C) vibrations are present in the IR and Raman spectra, as expected for a non-linear C–Sn–C fragment, in positions close to those found in the equivalent PN-2H derivatives [5].

The parameters of the Mössbauer spectra collected at 80 K are summarized in the Experimental Part. All the spectra consist of well resolved, slightly asymmetric doublets with isomer shift and quadrupole splitting values that are typical for diorganotin(IV) compounds. As far as the isomer shift is concerned, the lutidine derivatives have values that are only slightly lower than those of the equivalent $[SnR_2(PN\text{-}2H)]$ complexes [5], a situation consistent with

the similarity of the donor fragment in both ligands. The QS values decrease regularly, as in the PN-2H complexes, from the methyl to the butyl compound.

The similarity of the vibrational pattern of the Lu-2H fragment in these three complexes provides evidence for the similar coordinative behaviour of the Lu ligand. On the other hand, the closeness of the Mössbauer parameters to those of the equivalent [SnR_2(PN-2H)] complexes suggests that the tin atom in the three compounds has a distorted tbp environment, equivalent to that found for this atom in [$SnBu_2$(Lu-2H)] [5].

The ligand, 2,6-lutidine-α^2,3-diol (Lu), was characterized by ^{1}H NMR spectroscopy in dmso-d_6 solution and the data are given in the Experimental Part. The signals were assigned on the basis of previously published data [2]. Due to the low solubility of the complexes in dmso, the spectrum of Lu was also acquired in MeOD and $CDCl_3$ along with those of the complexes.

The spectrum of compound **1** in $CDCl_3$ is complicated by the presence of more than one signal for each proton, a situation that indicates an equilibrium phenomenon in this solvent that was not detected for compounds **2** and **3** or in any of the spectra of the three compounds run in MeOD.

A signal attributable to H(O1) or H(O2) was not found in any of the solvents studied, an observation consistent with the bideprotonation of the ligand. The peak assigned to C(8)H_2 in each of the spectra of compounds **2** and **3** in $CDCl_3$ and compound **3** in MeOD were flanked by satellites corresponding to coupling of these protons with the tin atom, $^3J(^1H–^{119}Sn) = 36$ Hz, showing that the solid state Sn–(O1) interaction remains in both solvents.

The spectrum of compound **1** in MeOD allowed us to obtain a value of 82 Hz for $^2J(^1H–^{119}Sn)$. When this value is substituted into the Lockhart–Manders equation (eq. 2) [22], a value of 133° was obtained for the CH_3–Sn–CH_3 angle. This value is narrower than that obtained (151.8°) for **1** · H_2O in the solid state and is indicative of the low ability of MeOD to be incorporated into the tin coordination kernel.

The ^{119}Sn NMR spectra of the complexes show two signals, which indicates the existence of slightly different organotin moieties in solution. The signals are shifted to slightly lower field with respect to the positions previously found for the equivalent [SnR_2(PN-2H)] complexes in DMSO-d_6 [5,23]. Although this value is influenced by several factors, it may be used to infer the coordination number of the tin atom [24,25]. All the values obtained are in the range reported [24] for pentacoordinate tin, even though the values found for the butyl derivative are also within the typical range for hexacoordinate tin compounds [25].

3.4. In vitro antitumor screening

A comparative analysis of the cytotoxic activity of these compounds with that of [$SnBu_2$(PN-2H)], which proved to be active against several cellular lines [4], was carried out.

Table 4
Results of *in vitro* cytostatic assays against the HeLa-229, A2780 and A2780cis cell lines

Compound	IC_{50} (μM)			RF[a]
	HeLa-229	A2780	A2780cis	
[$SnBu_2$(Lu-2H)]	1.29 ± 0.03	0.61 ± 0.1	1.5 ± 0.3	2.45
[$SnBu_2$(PN-2H)]	0.6 ± 0.5	0.24 ± 0.15	0.24 ± 0.1	1.0
Cisplatin	0.53 ± 0.06	0.47 ± 0.4	3.6 ± 0.6	7.66

[a] The resistance factor: RF = IC_{50}(A2780cis)/IC_{50}(A2780).

The activities of Lu, PN, the three [SnR_2(Lu-2H)] complexes and three equivalent [SnR_2(PN-2H)] complexes were assessed, with cisplatin as a reference, against HeLa-229, A2780 and A2780cis cell lines. The Lu and PN ligands (despite PN is active against the hepatoma cell line HepG2 [26], the human pancreatic carcinoma cell line PANC-1 [27] and the feline mammary tumour cell line FRM [28]) showed a low activity and, as in other cases [29], the activities of the complexes decreased as the size of the R substituent decreased; the Me and Et derivatives had a low activity that made determination of the IC_{50} value unwarranted.

The IC_{50} values (μM) for [$SnBu_2$(Lu-2H)], [$SnBu_2$(PN-2H)] and cisplatin are shown in Table 4. As can be seen, the values for [$SnBu_2$(PN-2H)] are better than those found for the equivalent lutidine compound and are also better than those of cisplatin against all the cellular lines tested. Of particular relevance in the search for alternatives to cisplatin is the comparison of the activity of the compounds against the A2780 and A2780cis cell lines. In the A2780cis line a decreased accumulation of cisplatin is observed along with enhanced repair tolerance and elevated glutathione levels compared with the parent A2780 cell line [30]. The decrease in activity shown by cisplatin against this line is less marked in the case of the Lu derivative (RF = 2.45) and particularly in the PN derivative (RF = 1), which also shows better values than the reference against both lines.

4. Conclusions

In this study, we prepared and characterized, both in the solid phase and in solution, the lutidine (Lu) complexes [SnR_2(Lu-2H)] (R = Me, Et, Bu). The coordinated groups of the ligand are the same and the structural features of the complexes resemble those of the pyridoxine compounds (PN, vitamin B_6). Whereas the Me and Et derivatives of both ligands show low cytotoxic activity against HeLa-229, A2780 and 2780cis cell lines, the complex [$SnBu_2$(PN-2H)] is significantly more active than the equivalent [$SnBu_2$(Lu-2H)] complex and also than cisplatin.

Acknowledgements

We thank the Xunta de Galicia, Spain, for support under Projects PGIDIT03PXIC20306PN and PGIDIT03-PXIC30103PN. F.C. thank the Spanish Agency for

International Cooperation and the University of Santiago de Compostela for Grants.

Appendix A. Supplementary material

CCDC 633210 and 633211 contain the supplementary crystallographic data for Lu and $\mathbf{1} \cdot H_2O$. These data can be obtained free of charge via http://www.ccdc.cam.ac.uk/conts/retrieving.html, or from the Cambridge Crystallographic Data Centre, 12 Union Road, Cambridge CB2 1EZ, UK; fax: (+44) 1223-336-033; or e-mail: deposit@ccdc.cam.ac.uk. Supplementary data associated with this article can be found, in the online version, at doi:10.1016/j.jorganchem.2007.04.004.

References

[1] (a) J.S. Casas, M.V. Castaño, M.S. García-Tasende, T. Perez Alvarez, A. Sánchez, J. Sordo, J. Inorg. Biochem. 61 (1996) 97;
(b) J.S. Casas, A. Castiñeiras, M.D. Couce, G. Martinez, J. Sordo, J.M. Varela, J. Organomet. Chem. 517 (1996) 165;
(c) J.S. Casas, E.E. Castellano, M.D. Couce, M.S. García-Tasende, A. Sánchez, J. Sordo, C. Taboada, E.M. Vázquez-López, Inorg. Chem. 40 (2001) 946;
(d) J.S. Casas, A. Castiñeiras, F. Condori, M.D. Couce, U. Russo, A. Sánchez, R. Seoane, J. Sordo, J.M. Varela, Polyhedron 22 (2003) 53;
(e) J.S. Casas, A. Castiñeiras, F. Condori, M.D. Couce, U. Russo, A. Sánchez, J. Sordo, J.M. Varela, Eur. J. Inorg. Chem. (2003) 2790.
[2] J.S. Casas, E.E. Castellano, F. Condori, M.D. Couce, A. Sánchez, J. Sordo, J.M. Varela, J. Zuckerman-Schpector, J. Chem. Soc, Dalton Trans. (1997) 4421.
[3] J.S. Casas, A. Castiñeiras, F. Condori, M.D. Couce, U. Russo, A. Sánchez, J. Sordo, J.M. Varela, Polyhedron 813 (2000) 813.
[4] M. Gielen, R. Willem, T. Mancilla, J. Ramharter, E. Joosen, Si, Ge, Sn, Pb Compd. IX (1986) 349.
[5] J.S. Casas, A. Castiñeiras, F. Condori, M.D. Couce, U. Russo, A. Sánchez, J. Sordo, J.M. Varela, E.M. Vázquez López, J. Organomet. Chem. 689 (2004) 620.
[6] R.S. Tobias, I. Ogrins, B.A. Nevett, Inorg. Chem. 1 (1962) 636.
[7] M. Kretschmar, GENHKLK Program for the Reduction of CAD4 Diffractometer Data, University of Tübingen, Germany, 1997.
[8] (a) G.M. Sheldrick, SADABS, University of Göttingen, Germany, 1996;
(b) A.C.T. North, D.C. Phillips, F.S. Mathews, Acta Crystallogr. A24 (1968) 351.
[9] G.M. Sheldrick, Acta Crystallogr. A46 (1990) 467.
[10] G.M. Sheldrich, SHELXL-97 Program for the refinement of crystal structures, University of Göttingen, Germany, 1997.
[11] International Tables for X-ray Crystallography. Vol. C, Kluwer Academic Plublishers, Dordrecht, The Netherlands, 1995.
[12] A.L. Spek, PLATON. A Multipurpose Crystallographic Tool, Utrecht University, Utrecht, The Netherlands, 1999.
[13] A.L. Spek, Acta Crystallogr. A46 (1990) C-34.
[14] W. Kueng, E. Silber, U. Eppenberger, Anal. Biochem. 182 (1989) 16.
[15] J. Longo, K.J. Franklin, M.F. Richardson, Acta Crystallogr. B38 (1982) 2721.
[16] T. Natsume, S. Aizawa, K. Hatamo, S. Funahashi, J. Chem. Soc., Dalton Trans. (1994) 2749, and references therein.
[17] A. Sánchez González, A. Castiñeiras, J.S. Casas, J. Sordo, U. Russo, Inorg. Chim. Acta 216 (1994) 257, and references therein.
[18] J.S. Casas, E.E. Castellano, M.D. Couce, J. Ellena, A. Sánchez, J.L. Sánchez, J. Sordo, C. Taboada, Inorg. Chem. 43 (2004) 1957.
[19] (a) K. Sakamoto, Y. Hamada, H. Akashi, A. Orita, J. Otera, Organometallics 18 (1999) 3555;
(b) K. Sakamoto, H. Ikeda, H. Akashi, T. Fukuyama, A. Orita, J. Otera, Organometallics 19 (2000) 3242.
[20] H. Lee, J.Y. Bae, O.-S. Kwon, S.J. Kim, S.D. Lee, H.S. Kim, J. Organomet. Chem. 689 (2004) 1816.
[21] H.L. Sing, A.K. Varshney, Main Group Met. Chem. 22 (1999) 529.
[22] T.P. Lockhart, W.F. Manders, Inorg. Chem. 25 (1986) 892.
[23] F. Kayser, M. Biesemans, M. Gielen, R. Willem, Magn. Res. Chem. 32 (1994) 358.
[24] J. Otera, J. Organomet. Chem. 221 (1981) 57.
[25] J. Holeček, M. Nádvorník, K. Handlíř, A. Lyčka, J. Organomet. Chem. 315 (1986) 229.
[26] A. Molina, T. Oka, S.M. Muñoz, M. Ghikamori-Aoyama, M. Kuwahata, Y. Natori, Nut. Cancer 28 (1997) 206.
[27] D.C. Plais, J. Gardner-Thorpe, H. Ito, S.W. Ashley, E.E. Whang, Nutr. Res. 23 (2003) 673.
[28] D. Shimada, A. Fukuda, H. Kanouchi, M. Matsumoto, T. Oka, Biosci. Biotechnol. Biochem. 70 (2006) 1038.
[29] M.I. Khan, M.K. Baloch, M. Ashfag, G. Stoter, J. Organomet. Chem. 691 (2006) 2554.
[30] J.M. Pérez, L.R. Kelland, E.I. Montero, F.E. Boxall, M.A. Fuertes, C. Alonso, C. Navarro-Ranninger, Mol. Pharm. 63 (2003) 933, and references therein.